

# Optimal Cooperative Power-Limited Rendezvous Between Coplanar Circular Orbits

Victoria Coverstone-Carroll and John E. Prussing

University of Illinois at Urbana-Champaign, Urbana, Illinois 61801-2935

Minimum-fuel rendezvous of two power-limited spacecraft is investigated. Both vehicles are active and provide thrust to complete the rendezvous. Total propellant consumption is minimized. A direct-minimization method, direct collocation with nonlinear programming, is used to obtain cooperative rendezvous solutions in an inverse-square gravitational field. Unconstrained and constrained circular terminal orbits are considered. The optimal solutions depend upon the power-to-mass ratios of the spacecraft, the initial orbits, and the specified transfer time. Optimal cooperative rendezvous solutions are compared with optimal active-passive solutions and with previously reported linearized solutions.

## Introduction

**H**ISTORICALLY, spacecraft rendezvous has involved one thrusting (active) vehicle and one coasting (passive) vehicle. A cooperative power-limited (PL) rendezvous is an orbital maneuver in which two PL spacecraft are active. With both vehicles thrusting, a reduction in total propellant consumption is obtained when compared to the traditional active-passive rendezvous. The practical application of cooperative rendezvous occurs if both vehicles have comparable size and propulsive capability. It would make no sense to consider cooperative rendezvous between a small spacecraft and a space station.

Early studies of cooperative control considered general linear or nonlinear systems with various performance indices.<sup>1–4</sup> Recently, cooperative rendezvous methodology has been applied to spacecraft maneuvering. Prussing and Conway<sup>5</sup> determined the optimal terminal maneuver for a cooperative impulsive rendezvous. Mirfakhraie<sup>6</sup> and Mirfakhraie and Conway<sup>7</sup> developed a method for determining fuel-optimal trajectories for the fixed-time impulsive cooperative rendezvous. Coverstone-Carroll and Prussing<sup>8</sup> obtained analytical solutions for fixed-time PL cooperative rendezvous using the Hill-Clohessy-Wiltshire linearized gravity field to approximate the inverse-square gravity field. In this article, fixed-time cooper-

ative and active-passive (noncooperative) rendezvous solutions are obtained for two PL spacecraft in an inverse-square gravity field. Transfer times, maximum exhaust powers, and the initial orbits of the spacecraft are varied to determine their influence on the optimal cooperative solution. Optimal solutions subject to circular terminal-orbit constraints are also examined.

## Necessary Conditions for Optimal Solution

Power-limited spacecraft have propulsion systems with an upper bound on the engine exhaust power  $P_{\max}$ . Typically, the value of  $P_{\max}$  is set by the limitations of a power source that is separate from the engines. The equations of motion for PL spacecraft subject to a single gravitational source along with an equation for the mass change along a thrusting trajectory are supplied by Prussing<sup>9</sup>:

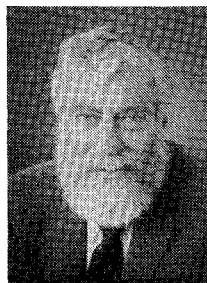
$$\ddot{\mathbf{r}} = \mathbf{g}(\mathbf{r}) + \mathbf{\Gamma} \quad (1)$$

$$\frac{1}{m(t)} - \frac{1}{m(t_0)} = \int_{t_0}^t \frac{\Gamma^2}{2P} dt \quad (2)$$

The variable  $\mathbf{r}$  is the position vector,  $\mathbf{g}(\mathbf{r})$  the gravitational acceleration vector,  $\mathbf{\Gamma}$  the thrust acceleration, and  $m$  the mass of the vehicle.



Victoria Coverstone-Carroll is an assistant professor of aeronautical and astronautical engineering at the University of Illinois at Urbana-Champaign. Her current research interests include optimal low-thrust spacecraft trajectories, optimal spacecraft attitude maneuvers, and spacecraft design. She was the recipient of the ZONTA Amelia Earhart Award and a NASA/ASEE Summer Faculty Fellow. She is a member of the American Astronautical Society and AIAA.



John E. Prussing is professor of aeronautical and astronautical engineering at the University of Illinois at Urbana-Champaign, where he has been a faculty member since 1969. He received his B.S. and M.S. degrees in 1963 in aeronautics and astronautics from the Massachusetts Institute of Technology and his Sc.D. in instrumentation from MIT in 1967. He is a past associate editor of the *Journal of Guidance, Control, and Dynamics* and is coauthor of the text *Orbital Mechanics*, published in 1993. He is a Fellow of the AIAA, has chaired the AIAA Astrodynamics Technical Committee, and was technical chairman of three AIAA astrodynamics conferences.

Equation (2) indicates that the final mass of a vehicle is maximized for a control history  $\Gamma(t)$  when the engine is operating at  $P_{\max}$  since any smaller exhaust power would result in a greater change in the total mass of the vehicle for the same trajectory satisfying the equations of motion (1).

For convenience a new variable,  $\alpha$ , the power-to-mass (PTM) ratio, is defined:

$$\alpha(t) = (P_{\max}/m(t)) \quad (3)$$

The introduction of the new variable  $\alpha$  allows Eq. (2) to be written as

$$\frac{d\alpha}{dt} = \frac{\Gamma^2}{2} \quad (4)$$

For a single vehicle, labeled vehicle  $i$ , define a state vector  $x_i$  of dimension  $7 \times 1$ ,  $x_i^T = [r_i^T \dot{r}_i^T \alpha_i]$ . The equation of motion for the  $i$ th vehicle can then be written in first-order form as

$$\dot{x}_i^T = f_i^T(x_i(t), \Gamma_i(t)) = [\dot{r}_i^T \quad g^T(r_i) + \Gamma_i^T \quad \frac{1}{2}\Gamma_i^T \Gamma_i] \quad (5)$$

For two active spacecraft, a combined state vector  $x$  of dimension  $14 \times 1$ ,  $x^T = [r_1^T \dot{r}_1^T \alpha_1 r_2^T \dot{r}_2^T \alpha_2] = [x_1^T x_2^T]$ , and control vector of dimension  $6 \times 1$ ,  $\Gamma^T = [\Gamma_1^T \Gamma_2^T]$ , is defined. The equations of motion then can be described by two sets of uncoupled equations, each of the form shown in Eq. (5):

$$\dot{x}^T = [f_1^T(x_1, \Gamma_1) \quad f_2^T(x_2, \Gamma_2)] = f^T(x(t), \Gamma(t)) \quad (6)$$

The objective of an optimal cooperative rendezvous is to transfer each vehicle from its initial orbit to a common final position and velocity in a given amount of time while maximizing the sum of the final masses of the spacecraft. Equation (7) relates this objective in terms of the reciprocal of the PTM ratios. The subscript  $f$  on a variable denotes the variable evaluated at the final time:

$$J = \sum_{i=1}^2 (m_{i0} - m_{if}) = \sum_{i=1}^2 \left( m_{i0} - \frac{P_{\max i}}{\alpha_{if}} \right) \quad (7)$$

To perform a rendezvous, the thrust acceleration vector of each vehicle must be determined. Using optimal control theory, it can be shown that, in any gravity field, the optimal thrust acceleration vector points in the direction opposite to the velocity costate vector for that vehicle.<sup>8</sup> Lawden<sup>10</sup> denotes the negative of the velocity costate vector as the primer vector  $p_i$ . Equation (8) provides the relationship between the optimal thrust acceleration vector and the primer vector<sup>8</sup>:

$$\Gamma_i = \frac{\alpha_{if}^2 p_i}{P_{\max i}} \quad (6 \text{ algebraic equations; } i = 1, 2) \quad (8)$$

### Primer Vector Differential Equation

The primer vector must be determined in order to integrate the equations of motion (1) for an optimal trajectory. In the inverse-square gravity field, the primer vector satisfies the following second-order homogeneous differential equation<sup>10</sup>:

$$\ddot{p}_i(t) = G(r_i)p_i(t) \quad i = 1, 2 \quad (9)$$

where

$$G(r_i) = \frac{\partial g(r_i)}{\partial r_i} = \frac{\mu}{r_i^5} [3r_i r_i^T - r_i^2 I_3] = G^T(r_i)$$

and  $I_3$  equals a  $3 \times 3$  identity matrix.

Here  $G(r)$  is the symmetric gravity gradient matrix. From Eq. (8) and (9) it is evident that the optimal trajectory never contains an intermediate coast arc. Because Eq. (9) is homogeneous, if the primer vector (and therefore the thrust) became identically zero, it would remain zero. Therefore, all PL optimal solutions exhibit continuous thrusting, in contrast to optimal constant-specific-impulse trajectories, which can contain intermediate coast arcs.

The 12 terminal boundary conditions for this second-order differential equation are

$$\begin{aligned} \dot{p}_i(t_f) &= \{(-1)^{(i+1)} \nu_1; i = 1, 2\} & (6 \text{ boundary conditions}) \\ p_i(t_f) &= \{(-1)^i \nu_2; i = 1, 2\} & (6 \text{ boundary conditions}) \end{aligned} \quad (10)$$

The values of the parameters  $\nu_1$  and  $\nu_2$  are determined by enforcing the terminal constraints involving the final position and velocity vectors of the vehicles. These six terminal constraints  $\psi[x(t_f)]$  are

$$\psi^T[x(t_f)] = (r_{1f}^T - r_{2f}^T, \dot{r}_{1f}^T - \dot{r}_{2f}^T) = 0 \quad (11)$$

Equations (1) and (9) along with their boundary conditions form a two-point boundary-value problem (TPBVP). The TPBVP associated with the inverse-square gravity field is highly nonlinear and an analytic solution is not available. The equation for an optimal PL trajectory derived in Ref. 9 is not directly applicable to the cooperative rendezvous problem. Total propellant must be minimized, which introduces coupling between the two individual vehicle solutions. Therefore, a method referred to as direct collocation with nonlinear programming (DCNLP)<sup>11</sup> is developed and used to determine the position, velocity, and PTM ratio histories for a cooperative rendezvous. DCNLP is referred to as a direct method because it minimizes the cost functional directly rather than using the (indirect) conditions from optimal control theory. After the direct method has converged to a solution, the necessary conditions are checked to determine if they are satisfied.

### Direct Collocation with Nonlinear Programming

DCNLP is a numerical method that has been used to solve many aerospace optimization problems.<sup>11-14</sup> This procedure transcribes the continuous equations of motion into a finite number of nonlinear equality constraints which must be satisfied at designated collocation points. These constraints must be satisfied if the discrete approximation is to accurately represent the actual states of the system. This method was originally developed by Dickmanns and Well<sup>12</sup> and used by Hargraves and Paris<sup>11</sup> to solve several atmospheric trajectory optimization problems. DCNLP was utilized to determine the optimal cooperative and active-passive rendezvous solutions.

### Constants of Motion

For the inverse-square gravity field, several constants of motion exist. The Hamiltonian, given by Eq. (12), is constant along an optimal trajectory<sup>8,15</sup>:

$$H = \sum_{i=1}^2 \left[ \dot{p}^T \dot{r}_i - p^T [g(r_i) + \Gamma_i] + \frac{1}{2} \lambda_{\alpha_i} \Gamma_i^T \Gamma_i \right] \quad (12)$$

Two vectors  $k_i$  are also constant along the optimal trajectory.<sup>15</sup> Equation (13) defines the  $k$  vector for each vehicle as

$$k_i = p_i \times \dot{r}_i - \dot{p}_i \times r_i \quad i = 1, 2 \quad (13)$$

Evaluating  $k_1$  and  $k_2$  at the final time leads to the fact that  $k_1 = -k_2$  for all times. These vectors are used to provide additional information on the accuracy of the solution. Using the output from DCNLP, the Hamiltonian and the  $k$  vectors computed at each collocation point and their constancy verifies that the necessary conditions are satisfied. The discrete approximation to the primer vector is obtained from the Lagrange multipliers in the nonlinear programming solution.

### Assumptions

A general optimal cooperative rendezvous solution is characterized by 15 parameters: two initial position and velocity vectors, two initial PTM ratios, and the total maneuver time. However, by restricting the initial orbits to be circular and coplanar, this number is reduced to 6: two initial-orbit radius magnitudes, a phase angle between the initial-orbit radius vectors, two initial PTM ratios, and the total maneuver time. A preliminary analysis was performed to study cooperative rendezvous using spacecraft with unequal initial

PTM ratios. However, optimal solutions were found to be more cooperative; i.e., both vehicles play a large part in the rendezvous, when the initial PTM ratios are equal. With unequal initial PTM ratios, one vehicle provides the majority of thrust and the optimal solution tends toward an active-passive rendezvous.<sup>16</sup> Therefore, to try to maximize the involvement of each vehicle, identical vehicles are assumed.

Power-limited vehicles with maximum exhaust power  $P_{\max}$  of  $10^7$  W and initial masses of 1000 kg are assumed. In the canonical units used for this study, vehicle 1 is initially in a circular orbit of radius 1 distance unit (DU) with an orbital period of  $2\pi$  time units (TU). Vehicle 2 is also initially in a circular orbit. The maximum exhaust power and initial mass previously stated translate to an initial PTM ratio of  $\alpha_0 = 0.129$  in Earth canonical units, 3.668 in lunar canonical units, and 56.6 in heliocentric canonical units. These three PTM ratios are used exclusively in this article.

### Circular Coplanar Rendezvous

With equal initial PTM ratios, the initial-orbit radius magnitudes can be specified and the initial PTM ratio  $\alpha_0$ , total rendezvous time  $T$ , and initial phase angle  $\phi_0$  between the two vehicles varied to investigate their influence on the optimal cooperative solution. The results are found to be consistent with the linearized results reported in Ref. 8. Table 1 shows the total amount of propellant consumed for both a cooperative and active-passive rendezvous along with the percentage of propellant saved by performing a cooperative rendezvous. Vehicle 2 is initially in a circular orbit of radius 2 DU. Since the gravity field is nonlinear, the cost of vehicle 1 performing the entire maneuver is not the same as the cost of vehicle 2. Therefore two noncooperative costs are displayed:  $J_c$  represents the cooperative cost,  $J_{nc1}$  represents the noncooperative cost when vehicle 1 is the active vehicle, and  $J_{nc2}$  is the noncooperative cost when vehicle 2 is active. The columns labeled %1 and %2 indicate the percentage of fuel saved by performing a cooperative rendezvous rather than an active-passive rendezvous with either vehicle 1 (%1) or vehicle 2 (%2) thrusting. Both vehicles begin the maneuver with an initial mass of 1 mass unit.

Table 1 shows that for a given maneuver (i.e., fixed  $T$  and  $\phi_0$ ), cooperative and active-passive costs decrease as  $\alpha_0$  increases. Table 1 also shows that cooperative rendezvous offers a larger savings in total propellant consumed over active-passive rendezvous as  $\alpha_0$  increases. Both concepts are illustrated through cases 1, 9, and 17. The cooperative and active-passive costs decrease as  $T$  increases, but the percentage of total propellant saved by performing a cooperative rendezvous does not always increase with increasing  $T$ , as is shown

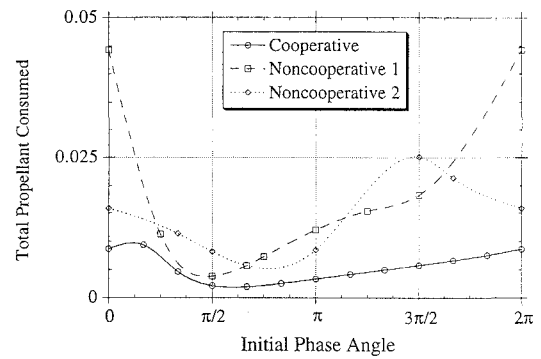


Fig. 1 Total propellant consumed vs phase angle;  $T = 2\pi$ ,  $\alpha_0 = 3.668$ .

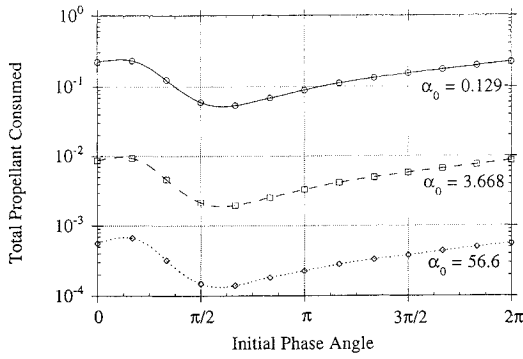
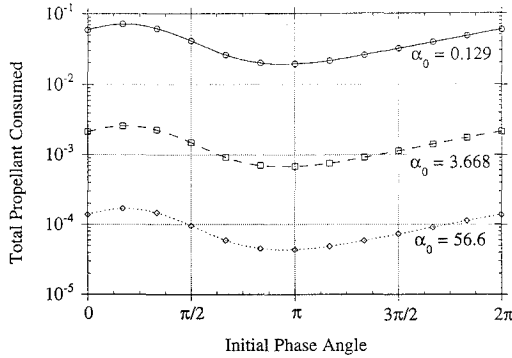
by comparing cases 2 and 6. Examining cases 1–4 reveals that the cooperative and active-passive costs do not necessarily increase with  $\phi_0$  but seem to achieve a minimum and maximum with respect to  $\phi_0$ . However, in all cases, cooperative rendezvous yields some savings in total propellant consumption over active-passive rendezvous.

Consider next Fig. 1, which displays the total propellant consumed during a cooperative and both active-passive rendezvous as a function of initial phase angle  $\phi_0$  between the two vehicles. The total maneuver time is  $2\pi$  TU. The initial PTM ratio of both vehicles is 3.668. A cubic spline fit has been used between calculated data points represented by symbols. Noncooperative 1 corresponds to the cost of the active-passive rendezvous where vehicle 1 performs the entire maneuver. Similarly, noncooperative 2 is the cost associated with vehicle 2 thrusting alone. Vehicle 2 is initially in a circular orbit of radius 2 DU. The phase angle between the vehicles is measured from vehicle 2 to vehicle 1 in the clockwise direction. Note that the cooperative cost is always less than either active or passive rendezvous.

Figures 2 and 3 display the cooperative costs for initial PTM ratios 0.129, 3.668, and 56.6. In Figs. 2 and 3 the total maneuver time is  $2\pi$  and  $3\pi$  TU, respectively. Note the similarities in the curves, in which the costs are plotted on a logarithmic scale. To understand the similarities in the cooperative cost curves, the terminal orbits are examined. Figures 4 and 5 display the semimajor axis and eccentricity of the terminal orbit as a function of initial phase angle for the total maneuver time of  $3\pi$  TU. For fixed-time rendezvous between given initial orbits, the semimajor axis and the eccentricity of the terminal orbits for a specified initial phase angle are very similar regardless of the initial PTM ratio. The similarity in the co-

Table 1 Cooperative and active-passive rendezvous total propellant consumption comparison

Case	$\alpha_0$	$\phi_0$	$T$	$J_c$	$J_{nc1}$	$J_{nc2}$	%1	%2
1	0.129	0	$2\pi$	0.2193498	0.5677561	0.3141013	61.4	30.2
2	0.129	$\pi/2$	$2\pi$	0.0584966	0.0978952	0.1892793	40.2	69.1
3	0.129	$\pi$	$2\pi$	0.0897844	0.2562255	0.1954603	65.0	54.1
4	0.129	$3\pi/2$	$2\pi$	0.1524876	0.3510911	0.4230510	56.6	64.0
5	0.129	0	$3\pi$	0.0592958	0.2165613	0.1999216	72.6	70.6
6	0.129	$\pi/2$	$3\pi$	0.0411624	0.0554056	0.0977820	25.7	57.9
7	0.129	$\pi$	$3\pi$	0.0191501	0.0543603	0.0498930	64.8	61.6
8	0.129	$3\pi/2$	$3\pi$	0.0315825	0.1524819	0.0691536	79.3	54.3
9	3.668	0	$2\pi$	0.0086388	0.0442548	0.0158501	80.5	45.5
10	3.668	$\pi/2$	$2\pi$	0.0021511	0.0038020	0.0081440	43.3	73.6
11	3.668	$\pi$	$2\pi$	0.0033196	0.0119708	0.0084718	72.3	60.8
12	3.668	$3\pi/2$	$2\pi$	0.0057721	0.0182800	0.0251390	68.4	77.0
13	3.668	0	$3\pi$	0.0021330	0.0096280	0.0087114	77.8	75.5
14	3.668	$\pi/2$	$3\pi$	0.0014858	0.0020586	0.0037971	27.8	60.8
15	3.668	$\pi$	$3\pi$	0.0006819	0.0020176	0.0018434	66.2	63.0
16	3.668	$3\pi/2$	$3\pi$	0.0011311	0.0062877	0.0026059	82.0	56.6
17	56.6	0	$2\pi$	0.0005620	0.0029918	0.0010426	81.2	46.1
18	56.6	$\pi/2$	$2\pi$	0.0001399	0.0002473	0.0005318	43.4	73.7
19	56.6	$\pi$	$2\pi$	0.0002156	0.0007846	0.0005534	72.5	61.0
20	56.6	$3\pi/2$	$2\pi$	0.0003746	0.0012052	0.0016684	68.9	77.5
21	56.6	0	$3\pi$	0.0001382	0.0006296	0.0005692	78.0	75.7
22	56.6	$\pi/2$	$3\pi$	0.0000961	0.0001337	0.0002458	28.1	60.9
23	56.6	$\pi$	$3\pi$	0.0000439	0.0001310	0.0001197	66.5	63.3
24	56.6	$3\pi/2$	$3\pi$	0.0000730	0.0004099	0.0001693	82.2	56.9

Fig. 2 Cooperative cost vs phase angle,  $T = 2\pi$ .Fig. 3 Cooperative cost vs phase angle,  $T = 3\pi$ .

operative cost curves seen in Figs. 2 and 3 is a consequence of the nearly identical terminal orbits, since the optimal trajectories vary little with respect to the initial PTM ratio.

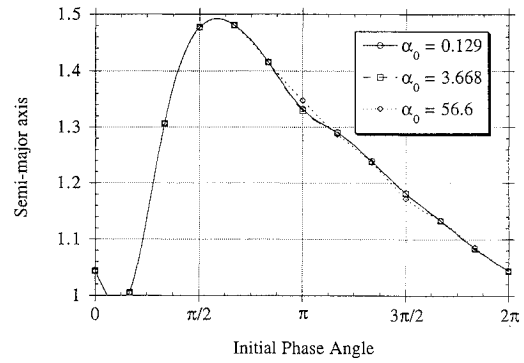
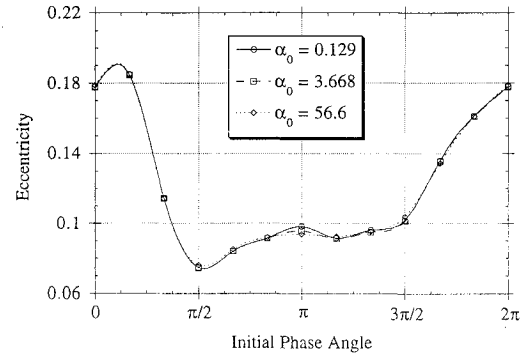
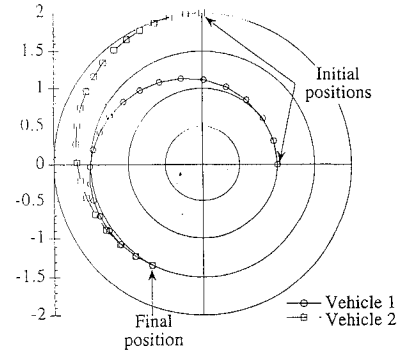
The optimal fixed-time active-passive rendezvous trajectories between specified orbits are invariant with respect to the initial PTM ratio of the vehicle. Therefore, cost curves for these maneuver appear similar in form for any initial PTM ratio. The relationship between the active-passive costs and the initial PTM ratios is easily understood from optimal control theory. For an active-passive rendezvous the optimal thrust acceleration vector  $\Gamma_{nc}$  is equal to the primer vector.<sup>10</sup> The primer vector satisfies a second-order homogeneous differential equation (9) whose boundary conditions are determined by enforcing the terminal constraints on the position and velocity vectors of the two vehicles. These constraints are functions of the initial positions and velocities of the vehicles and the total maneuver time and are independent of the PTM ratios. Therefore, for an active-passive rendezvous the primer vector and hence the optimal thrust acceleration vector  $\Gamma_{nc}$  depends only on the initial positions and velocities of the vehicles and on the total maneuver time. Once an optimal noncooperative solution has been obtained for given initial positions and velocities of the vehicles, total maneuver time, and initial PTM ratio, the optimal noncooperative solution is known for all initial PTM ratios. Equation (14) can be used to obtain the final PTM ratio and hence the final mass of the thrusting vehicle through the constant  $K_{nc}$ :

$$\begin{aligned} \Delta\alpha &= \alpha_f - \alpha_0 = \frac{1}{2} \int_0^{t_f} \Gamma_{nc}^T(\tau) \Gamma_{nc}(\tau) d\tau \\ &= \frac{1}{2} \int_0^{t_f} p^T(\tau) p(\tau) d\tau = K_{nc} \end{aligned} \quad (14)$$

Define  $J_{nc}$  as the total propellant consumed for a noncooperative rendezvous. Then  $J_{nc}$  may be written in terms of  $K_{nc}$ , the initial maximum exhaust power  $P_{max}$ , and the PTM ratio  $\alpha_0$  of the thrusting vehicle as

$$J_{nc} = \frac{P_{max} K_{nc}}{\alpha_0 (K_{nc} + \alpha_0)} \quad (15)$$

Equation (16) relates total propellant consumption to initial PTM ratio for a given active-passive rendezvous. Let  $J_{nc-}$  represent

Fig. 4 Semimajor axis of terminal orbit vs phase angle,  $T = 3\pi$ .Fig. 5 Eccentricity of terminal orbit vs phase angle,  $T = 3\pi$ .Fig. 6 Cooperative rendezvous position trajectories;  $\phi_0 = \pi/2$ ,  $T = 2\pi$ .

the total propellant consumed to perform the noncooperative rendezvous with the initial PTM ratio of the active vehicle denoted by  $\alpha_{0-} = P_{max} - m_{0-}$ . The total propellant consumed  $J_{nc+}$  with a different PTM ratio  $\alpha_{0+} = P_{max} - m_{0+}$  is then obtained through Eq. (16), which was used to generate the noncooperative costs for cases 9–24 of Table 1 from the active-passive costs of cases 1–8:

$$J_{nc+} = m_{0+} - \frac{P_{max+}(m_{0-} - J_{nc-})}{(\alpha_{0+} - \alpha_{0-})(m_{0-} - J_{nc-}) + P_{max-}} \quad (16)$$

Figures 6–10 are the cooperative and active-passive rendezvous position trajectories, thrust acceleration magnitude, and angle histories for an initial phase angle of  $\pi/2$  rad. The total maneuver time is  $2\pi$  TU and the initial PTM ratio is 0.129. Cooperative and noncooperative rendezvous solutions for the initial PTM ratios of 3.668 and 56.6 are not shown due to the similarity in the solutions. The control angles  $\theta$  are measured with respect to the inertial frame shown in the position trajectory figures, where the  $x$  coordinate is measured along the abscissa,  $y$  along the ordinate, and  $\theta = \tan^{-1}(\Gamma_y/\Gamma_x)$ . Note that the cooperative rendezvous requires smaller thrust magnitudes from the engines than do either active or passive rendezvous. The production of large thrust accelerations could require more propellant than is available to the vehicle. Therefore, since smaller thrust accelerations are required for the cooperative rendezvous, maneuvers

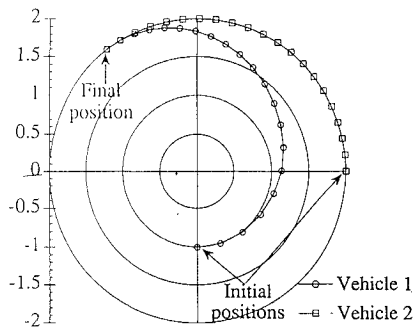


Fig. 7 Noncooperative rendezvous position trajectories; vehicle 1 provides thrust;  $\phi_0 = \pi/2$ ,  $T = 2\pi$ .

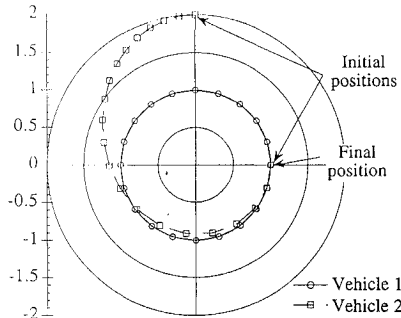


Fig. 8 Noncooperative rendezvous position trajectories; vehicle 2 provides thrust;  $\phi_0 = \pi/2$ ,  $T = 2\pi$ .

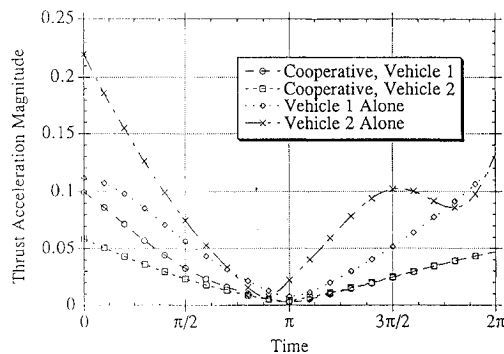


Fig. 9 Thrust acceleration magnitude history;  $\phi_0 = \pi/2$ ,  $T = 2\pi$ .

that may not be feasible with just one active vehicle may become feasible through cooperative thrusting.

Figure 10 illustrates that at the final time the two thrust acceleration vectors point in opposite directions. This observation results from a necessary condition for an optimal control history.<sup>8</sup> Equation (8) states that the optimal thrust acceleration vector of each vehicle is in the direction of its primer vector. Furthermore, the primer vectors of the two vehicles are equal in magnitude and opposite in direction at the final time. Thus, the optimal thrust acceleration vectors for the two vehicles must be in opposite directions at the final time. The magnitudes of the controls at the final time do not necessarily have to be equal since they are scaled with respect to the final primer vector magnitude, as seen in Eq. (8).

As the total rendezvous time or the initial PTM ratio is decreased, an optimal cooperative rendezvous tends toward an active-passive rendezvous. This phenomenon occurs due to the fact that, as the maneuver becomes more demanding (less total time or lower initial PTM ratios), larger thrust accelerations are required to complete the rendezvous, resulting in increased propellant consumption. As a vehicle loses propellant, it becomes lighter, and thereby the maximum exhaust power seems more effective, leading to the engine appearing more efficient. Therefore, in demanding situations, instead of two equally inefficient vehicles largely contributing to the maneuver, it becomes optimal for one vehicle to perform nearly all the thrusting since it becomes increasingly efficient as it uses more propellant.

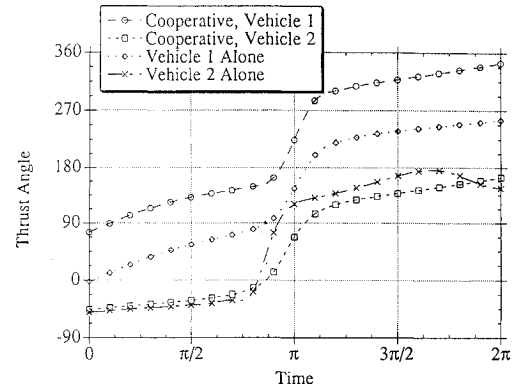


Fig. 10 Thrust direction history;  $\phi_0 = \pi/2$ ,  $T = 2\pi$ .

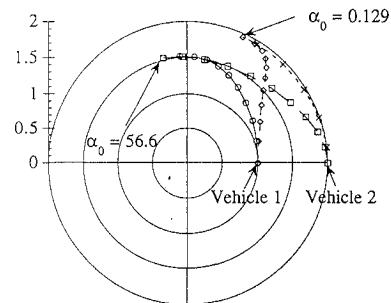


Fig. 11 Cooperative rendezvous position trajectories;  $\phi_0 = 0$ ,  $T = \pi$ .

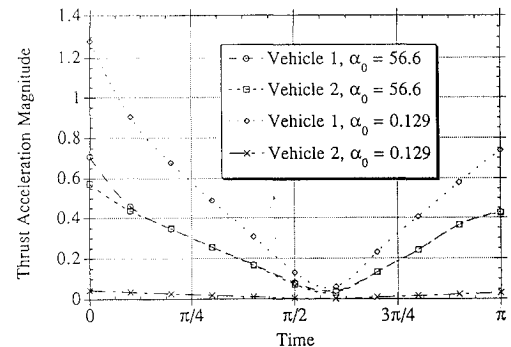


Fig. 12 Thrust acceleration history;  $\phi_0 = 0$ ,  $T = \pi$ .

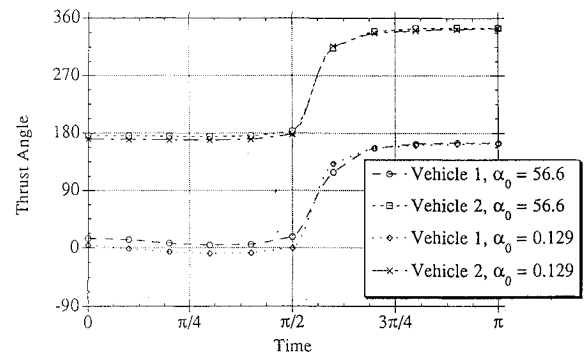


Fig. 13 Thrust direction history;  $\phi_0 = 0$ ,  $T = \pi$ .

This was found analytically for the impulsive case by Prussing and Conway.<sup>5</sup>

Figures 11–13 illustrate the paradox described above. Figure 11 shows the position trajectories for a cooperative rendezvous from an initial phase angle of zero radians and with a total maneuver time of  $\pi$  TU. The initial PTM ratios of 56.6 and 0.129 were used. The total amount of propellant consumed for the initial PTM of 56.6 is 0.0050316 mass units, and the final orbit has a semimajor axis of 1.567359 DU with an eccentricity of 0.0689626. The total amount of propellant consumed for the initial PTM of 0.129

increases to 0.8020212 mass units. The final orbit has a semimajor axis of 1.966009 DU with an eccentricity of 0.0076167. Both control histories require large accelerations, as seen in Fig. 12; however, for the initial PTM of 56.6 both vehicles perform about half of the maneuver. The cooperative rendezvous for the PTM ratio of 0.129 is very similar to the active-passive rendezvous where vehicle 1 is active. For this case, the thrust acceleration magnitude of vehicle 1 is extremely large and may be infeasible for low-thrust engines. Figure 13 shows the thrust angle profile, which is very similar for both rendezvous. All of the numerical results obtained are consistent with the linearized, neighboring orbit results reported in Ref. 8.

### Terminal Orbit Constraints

A cooperative rendezvous between coplanar circular orbits in an inverse-square gravity field typically does not result in a circular terminal orbit. However, since the initial orbits of both vehicles are circular, a circular terminal orbit may be desirable. The addition of constraints to ensure a circular terminal orbit and how these constraints affect the optimal cooperative rendezvous solution are now considered.

Analytic solutions to the unconstrained cooperative rendezvous in the inverse-square gravity field do not exist, and as previously described, DCNLP was used to compute the propellant-minimizing trajectories. To guarantee a circular terminal orbit, two nonlinear constraints [Eqs. (17) and (18)] must be added to the nonlinear programming problem. Equation (17) forces the final position and velocity vectors of the vehicles to be orthogonal whereas Eq. (18) ensures that the circular orbit relationship between the magnitudes of the final position and velocity is satisfied:

$$\mathbf{r}^T(T)\mathbf{v}(T) = 0 \quad (17)$$

$$v^2(T) = (1/r(T)) \quad (18)$$

To illustrate a constrained cooperative rendezvous, consider a rendezvous where vehicle 2 is in a circular orbit of radius 2 DU and vehicle 1 is in a circular orbit of radius 1 DU. The vehicles are assumed to be identical with an initial PTM ratio of 0.129. The total maneuver time remains at  $2\pi$  TU. The phase angle  $\phi$  between the vehicles is again varied. Figure 14 displays total propellant consumption as a function of the initial phase angle between the vehicles for the constrained cooperative rendezvous along with the total amount of propellant consumed for the unconstrained cooperative and both active-passive rendezvous. As expected, the cost associated with a constrained final orbit is greater than the unconstrained rendezvous but is less than both of the unconstrained active-passive rendezvous costs.

Figure 15 shows the semimajor axis of both constrained and unconstrained rendezvous. All computed semimajor axes corresponding to the unconstrained rendezvous fall between the two initial orbit semimajor axes of 1 and 2 DU. For the majority of initial phase angles, the constrained terminal-orbits semi major axes also lie in this range.

Figures 16 and 17 display the trajectories for the unconstrained and the constrained cooperative rendezvous for an initial phase angle of  $3\pi/2$  rad. The optimal constrained terminal orbit has a semimajor axis of approximately 1 DU, which roughly corresponds to the

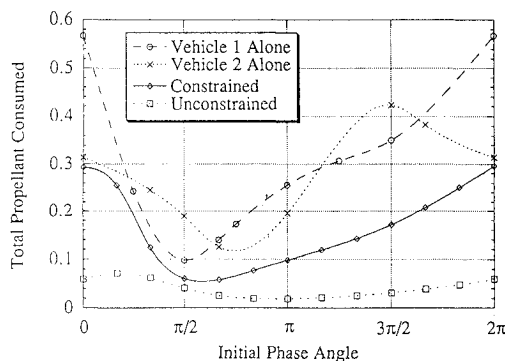


Fig. 14 Total propellant consumption vs initial phase angle.

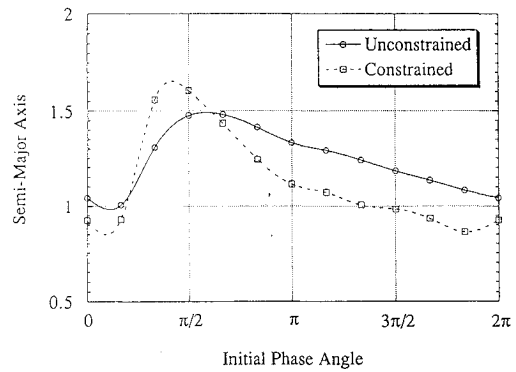


Fig. 15 Semimajor axis vs initial phase angle.

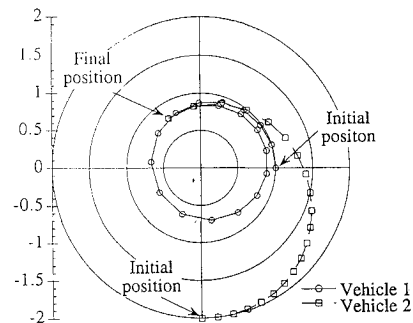


Fig. 16 Trajectories for unconstrained cooperative rendezvous,  $\phi_0 = 3\pi/2$ .

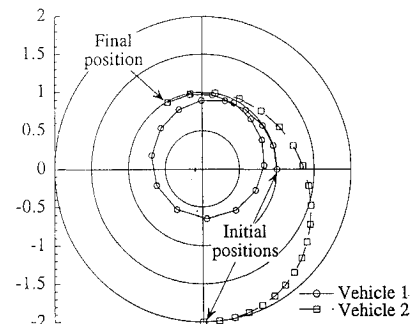


Fig. 17 Trajectories for constrained cooperative rendezvous,  $\phi_0 = 3\pi/2$ .

initial orbit of vehicle 1. However, this does not mean that vehicle 2 provides all the thrusting. Both vehicles actively participate in the maneuver. The associated constrained cooperative cost seen in Fig. 14 is considerably less than both noncooperative costs.

### Conclusions

Some general trends are exhibited for both cooperative and active-passive rendezvous in the inverse-square gravity field. First, as total maneuver time is increased, total propellant consumption for both cooperative and noncooperative rendezvous decreases. Also, as the initial PTM ratio increases, the relative efficiencies of the engines increase and the total amount of propellant consumed for both cooperative and noncooperative rendezvous decreases. In all cases, the cooperative rendezvous used less total propellant than the corresponding active-passive rendezvous; however, the percent savings in propellant is dependent on the total maneuver time, the initial phase angle, and the initial PTM ratio of the vehicles. These results are qualitatively similar to those obtained for the impulsive thrust problem. The addition of circular terminal-orbit constraints increases total propellant consumption when compared to the unconstrained cooperative rendezvous; however, this consistently yields lower total propellant consumption when compared to either active or passive rendezvous. The results presented represent an extension of previously reported linearized results to the inverse-square gravitational field.

## Acknowledgments

This research was partially supported by an Amelia Earhart Fellowship sponsored by the ZONTA International Foundation and by a NASA Space Grant Fellowship.

## References

- <sup>1</sup>Meschler, P. A., "Time-Optimal Rendezvous Strategies," *IEEE Transactions on Automatic Control*, Vol. 8, Oct. 1963, pp. 279–282.
- <sup>2</sup>Giesekeing, K. L., "Optimal Control of Co-operative Systems: The Rendezvous Problem," Report R-218 UIUC CSL, 1964.
- <sup>3</sup>Carter, T. E., "A Simple Feedback Law for a Cooperative Rendezvous Problem," NASA TM X-53568, Oct. 1966.
- <sup>4</sup>Kahne, S. J., "Optimal Cooperative State Rendezvous and Pontryagin's Maximum Principle," Air Force Cambridge Research Laboratories AFCRL-65-233, Apr. 1965.
- <sup>5</sup>Prussing, J. E., and Conway, B. A., "Optimal Terminal Maneuver for a Cooperative Impulsive Rendezvous," *Journal of Guidance, Control, and Dynamics*, Vol. 12, No. 3, 1989, pp. 433–435.
- <sup>6</sup>Mirfakhraie, K., "Optimal Cooperative Time-Fixed Impulsive Rendezvous," Ph.D. Dissertation, Univ. of Illinois at Urbana-Champaign, Urbana, IL, 1991.
- <sup>7</sup>Mirfakhraie, K., and Conway, B. A., "Optimal Cooperative Time-Fixed Impulsive Rendezvous," AIAA Paper 90-2962, Aug. 1990.
- <sup>8</sup>Coverstone-Carroll, V., and Prussing, J. E., "Optimal Power-Limited Rendezvous Between Neighboring Circular Orbits," *Journal of Guidance, Control, and Dynamics*, Vol. 16, No. 6, 1993, pp. 1045–1054.
- <sup>9</sup>Prussing, J. E., "Equation for Optimal Power-Limited Spacecraft Trajectories," *Journal of Guidance, Control and Dynamics*, Vol. 16, No. 2, 1993, pp. 391–393.
- <sup>10</sup>Lawden, D. F., *Optimal Trajectories for Space Navigation*, Butterworths, London, 1963.
- <sup>11</sup>Hargraves, C. R., and Paris, S. W., "Direct Trajectory Optimization Using Nonlinear Programming and Collocation," *Journal of Guidance and Control*, Vol. 10, No. 4, 1987, pp. 338–342.
- <sup>12</sup>Dickmanns, E. D., and Well, H., "Approximate Solution of Optimal Control Problems Using Third-Order Hermite Polynomial Functions," *Proceedings of the 6th Technical Conference on Optimization Techniques*, Springer-Verlag, New York, IFIP-TC7 1975.
- <sup>13</sup>Enright, P. J., and Conway, B. A., "Optimal Finite-Thrust Spacecraft Trajectories Using Collocation and Nonlinear Programming," *Journal of Guidance, Control, and Dynamics*, Vol. 14, No. 5, 1991, pp. 981–985.
- <sup>14</sup>Enright, P. J., and Conway, B. A., "Discrete Approximations to Optimal Trajectories Using Direct Transcription and Nonlinear Programming," *Journal of Guidance, Control, and Dynamics*, Vol. 15, No. 4, 1992, pp. 994–1002.
- <sup>15</sup>Marec, J.-P., *Optimal Space Trajectories*, Elsevier Scientific, Amsterdam, 1979.
- <sup>16</sup>Coverstone-Carroll, V., "Optimal Cooperative Power-Limited Rendezvous," Ph.D. Dissertation, Univ. of Illinois at Urbana-Champaign, Urbana, IL, 1992.